# Pharmacodynamic, pharmacokinetic and rat brain receptor occupancy profile of NLX-112, a highly selective 5-HT 1A receptor biased agonist

Ronan Y Depoortère, Andrew C Mccreary, Benjamin Vidal, Mark A Varney, Luc Zimmer, Adrian Newman-Tancredi

▶ **To cite this version:**

Ronan Y Depoortère, Andrew C Mccreary, Benjamin Vidal, Mark A Varney, Luc Zimmer, et al.. Pharmacodynamic, pharmacokinetic and rat brain receptor occupancy profile of NLX-112, a highly selective 5-HT 1A receptor biased agonist. Naunyn-Schmiedeberg's Archives of Pharmacology, 2024, 398 (1), pp.991-1002. ⟨10.1007/s00210-024-03323-0⟩. ⟨hal-04932477v1⟩

**HAL Id: hal-04932477**

**https://hal.science/hal-04932477v1**

Submitted on 6 Feb 2025 (v1), last revised 6 Feb 2025 (v2)

**HAL** is a multi-disciplinary open access archive for the deposit and dissemination of scientific research documents, whether they are published or not. The documents may come from teaching and research institutions in France or abroad, or from public or private research centers.

L'archive ouverte pluridisciplinaire **HAL**, est destinée au dépôt et à la diffusion de documents scientifiques de niveau recherche, publiés ou non, émanant des établissements d'enseignement et de recherche français ou étrangers, des laboratoires publics ou privés.

HAL Authorization

# Metadata of the article that will be visualized in OnlineFirst

| | | |
|---|---|---|
| ArticleTitle | Pharmacodynamic, pharmacokinetic and rat brain receptor occupancy profile of NLX-112, a highly selective 5-$HT_{1A}$ receptor biased agonist | |
| Article Sub-Title | | |
| Article CopyRight | The Author(s), under exclusive licence to Springer-Verlag GmbH Germany, part of Springer Nature (This will be the copyright line in the final PDF) | |
| Journal Name | Naunyn-Schmiedeberg's Archives of Pharmacology | |
| Corresponding Author | FamilyName | **Newman-Tancredi** |
| | Particle | |
| | Given Name | **Adrian** |
| | Suffix | |
| | Division | |
| | Organization | Neurolixis SAS |
| | Address | 2 Rue Georges Charpak, 81100, Castres, France |
| | Phone | |
| | Fax | |
| | Email | anewmantancredi@neurolixis.com |
| | URL | |
| | ORCID | |
| Author | FamilyName | **Depoortère** |
| | Particle | |
| | Given Name | **Ronan Y.** |
| | Suffix | |
| | Division | |
| | Organization | Neurolixis SAS |
| | Address | 2 Rue Georges Charpak, 81100, Castres, France |
| | Phone | |
| | Fax | |
| | Email | |
| | URL | |
| | ORCID | |
| Author | FamilyName | **McCreary** |
| | Particle | |
| | Given Name | **Andrew C.** |
| | Suffix | |
| | Division | |
| | Organization | Brains On-Line |
| | Address | Groningen, Netherlands |
| | Division | |
| | Organization | GW Pharmaceuticals |
| | Address | Cambridge, UK |
| | Phone | |
| | Fax | |
| | Email | |
| | URL | |
| | ORCID | |
| Author | FamilyName | **Vidal** |

| | | |
|---|---|---|
| | Particle | |
| | Given Name | **Benjamin** |
| | Suffix | |
| | Division | |
| | Organization | Université Claude Bernard Lyon 1, Lyon Neuroscience Research Center, CNRS, INSERM, CERMEP-Imaging Platform |
| | Address | Bron, France |
| | Phone | |
| | Fax | |
| | Email | |
| | URL | |
| | ORCID | |
| Author | FamilyName | **Varney** |
| | Particle | |
| | Given Name | **Mark A.** |
| | Suffix | |
| | Division | |
| | Organization | Neurolixis SAS |
| | Address | 2 Rue Georges Charpak, 81100, Castres, France |
| | Phone | |
| | Fax | |
| | Email | |
| | URL | |
| | ORCID | |
| Author | FamilyName | **Zimmer** |
| | Particle | |
| | Given Name | **Luc** |
| | Suffix | |
| | Division | |
| | Organization | Université Claude Bernard Lyon 1, Lyon Neuroscience Research Center, CNRS, INSERM, CERMEP-Imaging Platform |
| | Address | Bron, France |
| | Division | |
| | Organization | Hospices Civils de Lyon |
| | Address | Lyon, France |
| | Phone | |
| | Fax | |
| | Email | |
| | URL | |
| | ORCID | |



| | | |
|---|---|---|
| Schedule | Received | 20 Mar 2024 |
| | Revised | |
| | Accepted | 22 Jul 2024 |



Abstract

NLX-112 (i.e., F13640, befiradol) exhibits nanomolar affinity, exceptional selectivity and full agonist efficacy at serotonin 5-$HT_{1A}$ receptors. NLX-112 shows efficacy in rat, marmoset and macaque models of L-DOPA induced dyskinesia (LID) in Parkinson's disease and has shown clinical efficacy in a Phase 2a proof-of-concept study for this indication. Here we investigated, in rats, its pharmacodynamic, pharmacokinetic (PK) and brain 5-$HT_{1A}$ receptor occupancy profiles, and its PK properties in the absence and presence of L-DOPA. Total and free NLX-112 exposure in plasma, CSF and striatal ECF was dose-proportional over the range tested (0.04, 0.16 and 0.63 mg/kg i.p.). NLX-112 exposure increased rapidly ($T_{max}$ 0.25–0.5h) and exhibited approximately threefold longer half-life in brain than in plasma (1.1 and 3.6h, respectively). At a pharmacologically relevant dose of 0.16 mg/kg i.p., previously shown to elicit anti-LID activity in parkinsonian rats, brain concentration of NLX-112 was 51–63 ng/g from 0.15 to 1h. In microPET imaging experiments, NLX-112 showed dose-dependent reduction of 18F-F13640 (i.e., 18F-NLX-112) brain 5-$HT_{1A}$ receptor labeling in cingulate cortex and

| | |
|---|---|
| | striatum, regions associated with motor control and mood, with almost complete inhibition of labeling at the dose of 0.63 mg/kg i.p.. Co-administration of L-DOPA (6 mg/kg s.c., a dose used to elicit LID in parkinsonian rats) together with NLX-112 (0.16 mg/kg i.p.) did not modify PK parameters in rat plasma and brain of either NLX-112 or L-DOPA. Here, we demonstrate that NLX-112's profile is compatible with 'druggable' parameters for CNS indications, and of the results provide measures of brain concentrations and 5-$HT_{1A}$ receptor binding parameters relevant to the anti-dyskinetic activity of the compound. |
| Keywords (separated by '-') | 5-$HT_{1A}$ receptors - Dyskinesia - NLX-112 - L-DOPA - Parkison's disease - Pharmacokinetics - Rat |
| Footnote Information | The online version contains supplementary material available at https://doi.org/10.1007/s00210-024-03323-0 . |

Naunyn-Schmiedeberg's Archives of Pharmacology
https://doi.org/10.1007/s00210-024-03323-0

RESEARCH

# Pharmacodynamic, pharmacokinetic and rat brain receptor occupancy profile of NLX-112, a highly selective 5-HT$_{1A}$ receptor biased agonist

Ronan Y. Depoortère[1] · Andrew C. McCreary[2,3] · Benjamin Vidal[4] · Mark A. Varney[1] · Luc Zimmer[4,5] · Adrian Newman-Tancredi[1]

Received: 20 March 2024 / Accepted: 22 July 2024
© The Author(s), under exclusive licence to Springer-Verlag GmbH Germany, part of Springer Nature 2024

## Abstract

NLX-112 (i.e., F13640, befiradol) exhibits nanomolar affinity, exceptional selectivity and full agonist efficacy at serotonin 5-HT$_{1A}$ receptors. NLX-112 shows efficacy in rat, marmoset and macaque models of L-DOPA induced dyskinesia (LID) in Parkinson's disease and has shown clinical efficacy in a Phase 2a proof-of-concept study for this indication. Here we investigated, in rats, its pharmacodynamic, pharmacokinetic (PK) and brain 5-HT$_{1A}$ receptor occupancy profiles, and its PK properties in the absence and presence of L-DOPA. Total and free NLX-112 exposure in plasma, CSF and striatal ECF was dose-proportional over the range tested (0.04, 0.16 and 0.63 mg/kg i.p.). NLX-112 exposure increased rapidly ($T_{max}$ 0.25–0.5h) and exhibited approximately threefold longer half-life in brain than in plasma (1.1 and 3.6h, respectively). At a pharmacologically relevant dose of 0.16 mg/kg i.p., previously shown to elicit anti-LID activity in parkinsonian rats, brain concentration of NLX-112 was 51–63 ng/g from 0.15 to 1h. In microPET imaging experiments, NLX-112 showed dose-dependent reduction of $^{18}$F-F13640 (i.e., $^{18}$F-NLX-112) brain 5-HT$_{1A}$ receptor labeling in cingulate cortex and striatum, regions associated with motor control and mood, with almost complete inhibition of labeling at the dose of 0.63 mg/kg i.p.. Co-administration of L-DOPA (6 mg/kg s.c., a dose used to elicit LID in parkinsonian rats) together with NLX-112 (0.16 mg/kg i.p.) did not modify PK parameters in rat plasma and brain of either NLX-112 or L-DOPA. Here, we demonstrate that NLX-112's profile is compatible with 'druggable' parameters for CNS indications, and of the results provide measures of brain concentrations and 5-HT$_{1A}$ receptor binding parameters relevant to the anti-dyskinetic activity of the compound.

**Keywords** 5-HT$_{1A}$ receptors · Dyskinesia · NLX-112 · L-DOPA · Parkison's disease · Pharmacokinetics · Rat

## Introduction

Serotonin (5-hydroxytriptamine, 5-HT) 1A (5-HT$_{1A}$) receptors are important targets for treatment of a variety of indications, e.g. depression and anxiety, acute and chronic pain, and movement disorders (Borroto-Escuela et al. 2021; Pagano et al. 2017; Celada et al. 2013; Barnes et al. 2021; Pourhamzeh et al. 2021). In movement disorders, such as Parkinson's disease (PD), activation of these receptors is associated with alleviation of motor dysfunctions in both animal models and human pathological states; for example, 5-HT$_{1A}$ receptor agonists such as 8-OH-DPAT, buspirone and ipsapirone attenuate haloperidol-induced catalepsy, a rat model of parkinsonian rigidity (Prinssen et al. 2002). In clinical trials, the early 5-HT$_{1A}$ receptor agonists, buspirone and sarizotan reduced dyskinesia in PD patients, who had received protracted treatment with L-DOPA (Levo 3,4-dihydroxyphénylalanine, the gold standard treatment for parkinsonism), but, unfortunately, also interfered with the anti-parkinsonian effects of the latter. This interference is likely due to the fact that these compounds also display antagonist activity at dopamine $D_2$ receptors, thus facilitating parkinsonism. Compounds such as buspirone also lack substantial agonist efficacy (they are partial agonists

✉ Adrian Newman-Tancredi
anewmantancredi@neurolixis.com

[1] Neurolixis SAS, 2 Rue Georges Charpak, 81100 Castres, France
[2] Brains On-Line, Groningen, Netherlands
[3] Present Address: GW Pharmaceuticals, Cambridge, UK
[4] Université Claude Bernard Lyon 1, Lyon Neuroscience Research Center, CNRS, INSERM, CERMEP-Imaging Platform, Bron, France
[5] Hospices Civils de Lyon, Lyon, France

UNCORRECTED PROOF

at 5-$HT_{1A}$ receptors), and are rapidly degraded to the active metabolite 1-(2-pyrimidinyl)piperazine (1-PP) (Caccia et al. 1983; Newman-Tancredi et al. 2022)).

Unlike older agonists, NLX-112 (a.k.a. F13640 or befiradol), shows a promising profile: it is exceptionally selective for and displays full agonist efficacy at 5-$HT_{1A}$ receptors (Newman-Tancredi et al. 2017), notably in brain regions associated with motor coordination (Vidal et al. 2020; Levigoureux et al. 2019; Newman-Tancredi et al. 2022). Moreover, NLX-112 is robustly active in animal models of abnormal motor behaviors. Hence, in rats rendered hemiparkinsonian by 6-OHDA lesioning of the nigrostriatal dopaminergic pathway, chronic treatment with L-DOPA produces abnormal involuntary movements (AIMs), considered to mimic L-DOPA-induced dyskinesia (LID) in PD patients. NLX-112 (0.01 to 0.16 mg/kg i.p.) potently and efficaciously reduced AIMs scores (Iderberg et al. 2015). Similarly, in non-human primates (marmosets and cynomolgus macaques) rendered parkinsonian-like by administration of the neurotoxin MPTP, and rendered dyskinetic with protracted treatment with L-DOPA, NLX-112 dose-dependently attenuated LID (Depoortere et al. 2020), (Fisher et al. 2020) (see Supplementary file for more in-depth description of LID, and the rationale for using NLX-112 to attenuate it). NLX-112 is currently under clinical development for treatment of LID in PD patients and successfully completed a proof-of-concept Phase 2a trial (ClinicalTrials.gov ID #NCT05148884) in which it met both its primary outcome of safety and tolerability, its secondary outcome of efficacy against LID and also diminished parkinsonian motor disability (Svenningsson et al. 2023).

Despite the fact that NLX-112 has been extensively investigated for its pharmacodynamic activity in a variety of animal models (see recent review by (Newman-Tancredi et al. 2022) for extended details), the relationship between its pharmacodynamic and its pharmacokinetic (PK) profiles has received limited attention. Hence, Bardin and collaborators (Bardin et al. 2005) reported data for total plasma exposure of NLX-112 (0.01 to 2.5 mg/kg i.p.), together with exposure measured from hippocampal microdialysate samples and compared it to behavioral effects in models of pain. However, they did not report free plasma exposure or, importantly, the levels of NLX-112 in the striatum, a brain structure involved in motor control and relevant to the development of NLX-112 for movement disorders.

The present study therefore investigated additional pharmacokinetic characteristics of NLX-112 after i.p. administration at pharmacologically active doses in male rats. Firstly, we explored the exposure levels of NLX-112 in plasma (total and free levels), in cerebrospinal fluid (total CSF levels) and in the striatum (free extra cellular fluid: ECF). Secondly, we undertook a microPET imaging study in which we explored the ability of unlabeled NLX-112 (administered i.p.) to displace binding of $^{18}$F-F13640 (i.e., $^{18}$F-labeled NLX-112), as a brain penetrant radiotracer to selectively label 5-$HT_{1A}$ receptors (Colom et al. 2021, 2020; Vidal et al. 2014, 2018). The goal was to estimate the level of 5-$HT_{1A}$ receptor occupancy at doses that produce anti-LID activity. Thirdly, we showed that co-administration of NLX-112 and L-DOPA did not alter the PK profiles of either of the compounds, supporting the conclusion that their effects are mediated independently of PK interactions. Overall, the present PK/PD and brain imaging study provides important exposure and target engagement information supporting the development of NLX-112 for LID.

## Methods

### Animals for drug exposure determinations

Total plasma, free blood (measured with ultraslow microdialysis, see below), total CSF and free striatal ECF exposure were determined in adult male Sprague–Dawley rats (weight 314–372 g, approximately 8 weeks old upon arrival in the laboratory, Harlan, the Netherlands), housed in polypropylene cages (40 X 50 X 20 $cm^3$) with wire mesh tops, in groups of 5 animals per cage. All animals had ad libitum access to standard rat chow (RMH-B 2181, HopeFarms BV, Woerden, NL) and tap water. Animals were housed in temperature (22 ± 2 °C) and humidity (55 ± 10%) controlled environment, using a 12-h light–dark cycle (lights on 07.00 – 19.00). Environmental enrichment was made available to all animals. All experiments were conducted in strict accordance with the National Institutes of Health "*Care and Use of Laboratory Animals*" guidelines, and with the Dutch law, and were approved by the Animal Care and Use Committee of the University of Groningen, the Netherlands.

A separate NLX-112/L-DOPA plasma and brain exposure study (alone and in combination) was carried out using adult male Sprague–Dawley rats (SLAC Laboratory Animal Co. Ltd., Shanghai, China). Animals were group-housed and acclimated for at least 3 days before being used. The animal room environment was controlled (20 to 26 °C, humidity 30 to 70%), 12 h artificial light and 12 h dark). Animals had ad libitum access to tap water and to Certified Rodent Diet (Beijing KEAO XIELI Feed Co., Ltd. Beijing, China) 4 h post dosing.

### Surgery for implantation of striatal microdialysis probes

Before surgery, Fynadine® (1 mg/kg s.c.) was administered to provide peri- and post-operative analgesia. Rats were anesthetized using isoflurane (2% and 500 mL/min O2), the anesthesia was maintained throughout the duration of

UNCORRECTED PROOF



Journal : Large 210 | Article No : 3323 | Pages : 12 | MS Code : 3323 | Dispatch : 29-7-2024

surgery. A mixture of excess topically applied bupivacaine (5 mg/mL) and epinephrine (5 µg/mL) was used for local anesthesia of the surgical sites. Rats were positioned into a stereotaxic apparatus (David Kopf Instruments, Tujunga, CA 91042, USA) for implantation with a MetaQuant ultraslow flow microdialysis probe (4 mm exposed microdialysate polyacrylonitrile membrane; Brainlink, Groningen, the Netherlands) in the striatum (coordinates: anterior + 0.6 mm from Bregma, lateral from midline -3.5 mm, ventral -7.5 mm from dura and the incisor-bar set to -3.3 mm for flat-skull position (Paxinos and Watson 2007).

## Surgery for cannulation of jugular and femoral veins and Cisterna Magna

Using a surgical procedure identical to that described above, a 10 cm segment of silicone tubing (0.64 mm ID; 0.94 mm OD, Brainlink, Groningen, the Netherlands) was inserted 4.2 mm deep from the point of venous insertion for the jugular vein and 2 mm deep for the femoral vein. Catheter patency was maintained by filling with 88% glycerol solution containing 500 IE/mL heparin.

For the Cisterna Magna, a cannula equipped with a dummy cannula, was inserted at the level of the occipital parietal junction (coordinates: on midline (0 mm), ventral -4.5 to 5.5 mm from the dura, with the incisor-bar set to 3.3 mm). When the cannula was inserted, tell-tale CSF flow was witnessed by the brief removal of the dummy cannula. Catheters, microdialysis probes and Cisterna Magna cannulae, were exteriorized following subcutaneous tunneling and affixed to the skull with dental cement and stainless-steel screws for additional stability.

In animals receiving a femoral vein catheter, an ultraslow flow microdialysis probe (MQ-JV-RC 800/040, with a 4.2 mm indwelling cannula; Brainlink, Groningen, the Netherlands) was also inserted into the jugular vein for the measurement of free plasma levels of NLX-112.

## Total and free plasma, total CSF and free striatum NLX-112 exposure by ultraslow microdialysis

All studies were conducted in awake, freely moving rats. For determination of total levels of NLX-112 in plasma the following procedure was followed. Sample preparation was carried out by mixing 5 µL of plasma sample with a 45 µL of a precipitation solution (16 mL acetonitrile, 3.78 mL ultrapurified water, 200 µL 1% ascorbic acid, 20 µL formic acid). This was vortexed for 10 s and after 5 min at room temperature was centrifuged at 13,000 rpm for 5 min at 4º C and 10 µL of the supernatant was added to 90 µL of a blank matrix (19.78 mL UP H2O, 20 µL formic acid and 200 µL 1% ascorbic acid).

For determination of free plasma, free striatum and total CSF levels of NLX-112, the following procedure was followed. Following microdialysis probe and cannula implantation and overnight recovery from surgery, the probes were connected to a microperfusion pump (Syringe pump, CMA, Sweden) and perfused with artificial CSF (147 mM NaCl, 3.0 mM KCl, 1.2 mM CaCl2, and 1.2 mM MgCl2, without 0.2% BSA). The flow rate was 0.12 µL/min with a carrier flow of 0.80 µL/min. After 60 min of pre-stabilization, microdialysis samples were collected at various time points between 0.25 and 4 h after drug administration (see Fig. 1). Samples were collected in tared mini-vials by an automated fraction collector maintained at 4ºC (TSE, Univentor, Malta). After collection of the samples, the vials were weighed again to determine sample volumes and stored at -80 °C until off-line analysis. Due to the volume of tubing and microdialysis probes, there was a latency in collecting microdialysate samples of approximately 30 and 11 min, in the jugular vein and striatum (ultraslow flow), respectively. Data are therefore shown corrected for this time-lag.

At the end of the experiment, the ultraslow flow was turned off, and after a period of 15 min, to allow the pressure to dissipate, two more samples were collected and weighed to verify proper functioning of the ultraslow microdialysis dialysis flow through the probe. Samples collected with ultraslow flow turned off should theoretically have less volume and therefore a lower mass. The difference in volume between the samples collected with ultraslow flow and those collected with ultraslow flow turned off indicates the actual rate of the ultraslow flow. This information was used for quality purposes only.

The different matrices obtained by the above procedures were analyzed by LC/MS/MS analysis as follows. Samples (5 µL aliquots) were injected onto an HPLC column using an automated sample injector (SIL20-AC-ht, Shimadzu, Japan). Chromatographic separation was performed on a MAX-RP; 3.0 × 100 mm, 2.5 µm column held at 35 °C. The mobile phases consisted of A: 0.1% formic acid (FA) in 2% ACN / 98% UP water and B: 0.1% FA in 90% ACN / 10% UP water at a flow rate of 0.30 mL/min. Mass spectrometric analyses were performed using an API 5000 MS/MS system consisting of an API 5000 MS/MS detector and a Turbo Ion Spray interface (Applied Biosystems, the Netherlands). The acquisitions were performed in positive ionization mode, with ion spray voltage set at 5.5 kV and a temperature of 600ºC. The instrument was operated in multiple-reaction-monitoring mode. Sample concentrations were determined by reference to calibration curves fitted using weighted (1/x) regression (csf) or quadratic fit (microdialysate and plasma). Concentrations were calculated with AnalystTM data system (Applied Biosystems, version 1.4.2, the Netherlands).

UNCORRECTED PROOF



Journal : Large 210 | Article No : 3323 | Pages : 12 | MS Code : 3323 | Dispatch : 29-7-2024

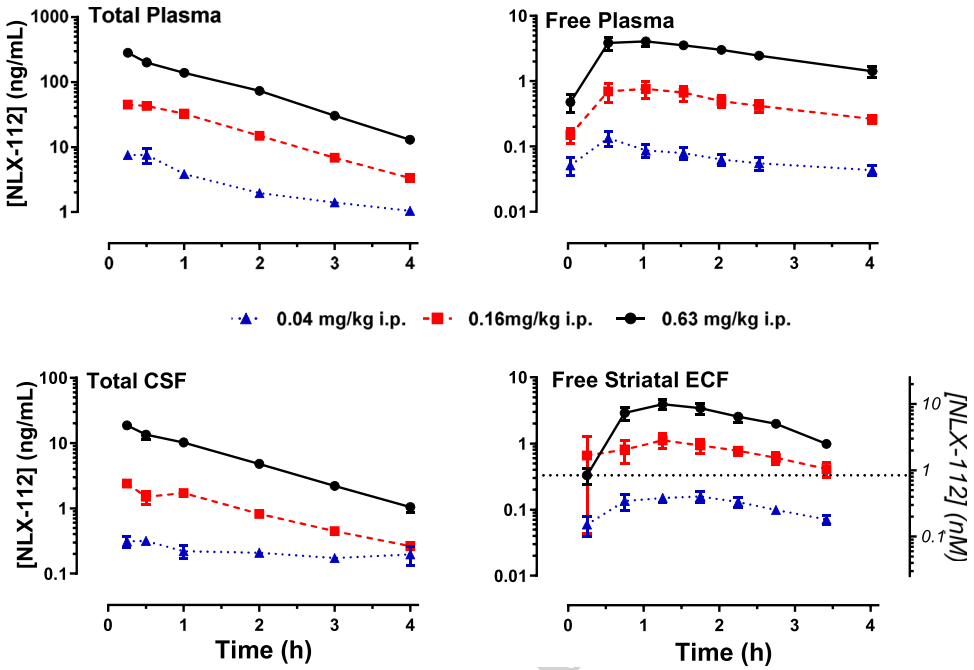


**Fig. 1** Dose & time dependency of NLX-112 levels in plasma, cerebrospinal fluid and striatal extracellular fluid. Symbols are mean ± SEM of NLX-112 concentration, expressed in ng/ml. Note that the Y axes scales are logarithmic. N = 5–6 rats per dose. The right-hand Y-axis in the 'Free striatal ECF' panel shows the concentration of NLX-112 in nM, and the dotted line indicates the in vitro affinity of NLX-112 for the rat 5-$HT_{1A}$ receptor ($K_i$: 0.85 nM) (Newman-Tancredi et al. 2022). CSF: cerebrospinal fluid; ECF: extracellular fluid

## Recovery indices of NLX-112 from the microdialysis probes

In vitro experiments were carried out to establish the percentage of recovery of NLX-112 across the microdialysis probe membrane. Microdialysis probes were placed in a beaker containing $10^{-8}$ M of NLX-112 in artificial CSF (same as above) in the presence of bovine serum albumin (BSA, 0.2%) in order to recapitulate the in vivo situation as closely as possible. The beaker contents were continuously stirred and maintained at 37 °C. The probes were perfused in the same manner as in the in vivo experiments, i.e., artificial CSF, but with and without 0.2% BSA. A set of six samples was collected per probe. Microdialysis studies were carried out at a slow flow of 0.8 µL/min and carrier flow of 0.12 µL/min. In a separate vial 120 µL of beaker content was diluted with 800 µL of ultrapurified water, replicating the dilution occurring within the MetaQuant microdialysis probes. In vitro recovery (%) was determined as the ratio between samples, following in vitro microdialysis, and the beaker content concentration.

## NLX-112 and L-DOPA exposure in plasma and brain following single or combined treatment

NLX-112 (0.16 mg/kg i.p.) and L-DOPA (6 mg/kg s.c.) were co-administered with the L-decarboxylase blocker benserazide (12 mg/kg s.c.). Blood samples were collected at various time points between 5 min and 4 h after drug administration (see Fig. 4) via cardiac puncture while the animals were under isoflurane anesthesia, with approximately 0.3 mL of blood collected at each time point. Following blood collection, brains were removed and homogenized with cold 10 mM PBS (w/v) using a Polytron (3 strokes or more until homogenous on wet ice, each 30 s), stored at -70 °C until LC/MS/MS analysis (below). Blood samples were processed for plasma by centrifugation at approximately 4 °C, 3000 g within 30 min of collection. Plasma samples were stored in polypropylene tubes, quickly frozen over dry ice and kept at -70 °C until LC/MS/MS analysis.

An aliquot of 40 µL of the plasma sample was protein precipitated with 160 µL of the internal standard, the mixture was vortex-mixed well and centrifuged at 4000 rpm for 20 min, 4 °C. 60 µL supernatant was then mixed with 120 µL water/MeOH (v:v, 75:25), vortex-mixed well and centrifuged at 4 °C. Chromatographic separation of a 5 µL sample was performed on an ACQUITY UPLC BEH C18 (2.1 × 50 mm, 1.7 µm) column held at 50 °C. The mobile phases consisted of A: 0.025% formic acid and 1 mM ammonium ethanoate in water/ACN (v:v, 95:5) and Mobile Phase B: 0.025% formic acid and 1 mM ammonium nitrate in acetonitrile/water (v:v, 95:5) at a flow rate of 0.6 mL/min. Following preparation of the brain samples (above) and chromatographic separation of a 5 µL sample, again using the ACQUITY UPLC BEH C18 (2.1 × 50 mm, 1.7 µm) column held at 50 °C. The mobile phases consisted of A: 0.025% formic acid and 1 mM ammonium acetate in water/acetonitrile (v:v, 95:5) and B: 0.025% formic acid and 1 mM ammonium acetate in acetone/water (v:v, 95:5) at a flow rate of 0.6 mL/min. Diclofenac was used as the internal standard for the plasma samples and 100 ng/mL labetalol, 100 ng/mL tolbutamide, and 200 ng/mL diclofenac in acetonitrile for the

UNCORRECTED



Journal : Large 210 | Article No : 3323 | Pages : 12 | MS Code : 3323 | Dispatch : 29-7-2024

brain samples. For the analysis of L-DOPA in plasma an aliquot of an aliquot of 10 µL sample was protein precipitated with 200 µL internal standard, the mixture was vortex-mixed well and centrifuged at 13000 rpm for 15 min, 20–25 °C. 200 µL supernatant was removed into another 96-well plate and evaporated to dry under nitrogen. The dried tube in 96-well plate was then reconstituted with 200 µL water with 0.1% formic acid, vortex-mixed and the plate centrifuged at 4 °C. 40 ng/mL acetaminophen and 40 ng/mL nizatidine in acetonitrile/methanol (v:v, 50:50) with 0.1% formic acid was used as the internal standard. Chromatographic separation of a 10 µL sample was performed using an Agilent Eclipse XDB-C18 4.6 × 100 mm, 3.5 µm) column at 20 °C with a flow rate of 0.85 mL/min following injection, with mobile phase consisting of A: 0.2% formic acid and 0.15% perfluoropropionic anhydride in water and B: methanol. For the analysis of L-DOPA brain homogenates an aliquot of 60 µL sample was protein precipitated with 240 µL of the internal standard, 40 ng/mL acetaminophen and 40 ng/mL and nizatidine in acetonitrile/methanol (v:v, 50:50) with 0.1% formic acid, the mixture was vortex-mixed well and centrifuged at 4000 rpm for 20 min at 4 °C. Chromatographic separation of a 8 µL was performed using an Agilent Eclipse XDB-C18 (4.6 × 100 mm, 3.5 µm) at 20 °C with a flow rate of 0.85 mL/min following injection of a 8.0 uL sample, with the mobile phase consisting of A: 0.2% FA & 0.15% perfluoropropionic anhydride in water and B: methanol.

In all cases mass spectrometric analyses were performed using API 4000 MS/MS system and concentrations calculated with reference to calibration a curve.

## In vivo occupancy of brain 5-HT$_{1A}$ receptors by NLX-112 (microPET imaging)

Male Sprague–Dawley rats (weight 270–480 g, Charles River, France) were anesthetized with 4% isoflurane, 1 L/min for 5 min (induction phase), and a catheter (24G, BD Insyte) was placed into their caudal vein. Anesthesia was then lowered to 2% isoflurane during the acquisition on a microPET/CT Inveon (Siemens, Germany), with monitoring of the respiratory rate thanks to a pressure sensor (Biovet, USA). The acquisition started with a CT image acquisition for 10 min, followed by the i.v. injection of 500 µL of $^{18}$F-F13640 (i.e., $^{18}$F-NLX-112) at 37 KBq/g (1 µCi/g) ± 10%. The radioactivity was measured in a series of 24 sequential frames of increasing duration from 20 s to 5 min. The total duration of the scan was 60 min. The images obtained were reconstructed in three dimensions. The regions of interest (ROIs: cingulate cortex, striatum, hippocampus, thalamus, brainstem and cerebellum) were automatically delineated thanks to an atlas dataset, after manual positioning of the PET images on an anatomical MRI template using the Inveon Research Workplace software (IRW, Siemens). The radioactivity was expressed in Bq/cm$^3$ and in SUVs (Standardized Uptake Value) by dividing the tissue radioactivity concentration by the injected dose of radioactivity per gram of animal. Rats underwent four microPET acquisitions with i.p. injection of saline or unlabeled NLX-112 at 0.04 mg/kg, 0.16 mg/kg or 0.63 mg/kg, 30 min before starting the scan, with a minimal interval of 48 h between two scans. The occupancy was estimated using the Lassen plot approach, which is required when there is no suitable reference region (as specific binding of $^{18}$F-F13640 is found in all the rat brain—see (Vidal et al. 2018)). For each dose, the differences $SUV_{baseline}$-$SUV_{competition}$ were calculated for all ROIs and plotted as a function of the baseline values, $SUV_{baseline}$. A linear regression was performed on the respective plots, to calculate the receptor occupancy given by the slope of the regression line (Cunningham et al. 2010; Takano et al. 2014).

## Data analysis

PK data were analyzed by non-compartmental approaches using the PKsolver® or Phoenix WinNonlin 6.3.0® software. The following parameters (units in parenthesis) were recorded:

- $C_{max}$: Maximal concentration observed (ng/mL for plasma; ng/g for brain)
- $T_{max}$: Time at which maximal concentration is observed (h)
- $T_{1/2}$: Terminal phase half-life (h).
- $AUC_{0\text{-last}}$: Area under the concentration–time curve up to the last measurable concentration (ng.h/mL for plasma; ng.h/g for brain)
- $AUC_{0\text{-last}}$ Ratio: The ratio of the $AUC_{0\text{-last}}$ from brain divided by that of the plasma

Data points on graphs show mean ± SEM values. Rat cohort size (n) is shown in Figure legends.

## In vitro activity at drug transporters

The in vitro activity of NLX-112 as a potential inhibitor or substrate was investigated at 8 different drug transporters: P-glycoprotein multidrug transporter (Pgp), Breast Cancer Resistance Protein (BCRP), Organo Anion Transporting Polypeptides 1B1 (OATP1B1) and 1B3 (OATP1B3), Organic Cation Transporter 1 (OCT1) and 2 (OCT2), Organic Anion Transporter 1 (OAT1) and 3 (OAT3). See Supplementary Table 1 for details of methodology and results.

UNCORRECTED PROOF



Journal : Large 210 | Article No : 3323 | Pages : 12 | MS Code : 3323 | Dispatch : 29-7-2024

## Drugs

NLX-112 (3-Chloro-4-fluorophenyl-[4-fluoro-4-([(5-methylpyridin-2-yl)methylamino] methyl)piperidin-1-yl]methanone, fumarate salt), base molecular weight: 393.9 g·mol$^{-1}$, salt molecular weight 509.9 g·mol$^{-1}$, was synthetized by O2Kem (Castres, France) and administered i.p. in a volume of 2 ml of saline/kg for the total and free plasma, total CSF and free striatum exposure experiment, and 1 ml/kg for the experiment in which NLX-112 and L-DOPA were combined. $^{18}$F-F13640 (i.e., $^{18}$F-NLX-112) radiosynthesis was performed by fluoro-nucleophilic substitution of a nitro-precursor following the method reported in (Vidal et al. 2018), and was administered in a 500 µL saline solution. L-DOPA and benserazide were obtained from commercial sources. Doses refer to the weight of the free base.

## Results

### Total and free plasma, total CSF and free striatal NLX-112 exposure

The in vitro microdialysis probe recovery studies showed that the NLX-112 recovery percentage was higher when Ringer's solution was used without, rather than with, 0.2% BSA (mean ± SEM: 78.2 ± 5.4% versus 43.3 ± 5.8%, respectively). BSA was therefore omitted for subsequent in vivo studies.

Data from the jugular and femoral vein were similar (data not shown) and were therefore pooled (see Total plasma, Fig. 1 and Table 1). Following i.p. administration, NLX-112 total (bound and unbound) plasma concentration was dose-proportional, with $C_{max}$: 282.6 ng/mL, for 0.63 mg/kg at 15 min; the $AUC_{0\text{-last}}$ at this latter dose was 360.0 ng*h/mL. $T_{1/2}$ was inversely proportional to the dose administered, and calculated as 0.87 h for 0.63 mg/kg.

Peak free (unbound) plasma concentrations were 60–70 times lower than those for total plasma and were observed at with $T_{max}$ values four times longer (1 h versus 15 min, for free plasma and total plasma, respectively) for 0.16 and 0.63 mg/kg. The $AUC_{0\text{-last}}$ values were 33–38 times lower than those calculated for total plasma; $T_{1/2}$ values were roughly twice as long as the total plasma ones.

Concerning the concentrations in the CSF, $C_{max}$ values were about 3 to 4 times higher than those for free plasma at 0.16 and 0.63 mg/kg and observed at earlier time-points; $AUC_{0\text{-last}}$ values were also notably higher by a factor of 2–3. Note that the $T_{1/2}$ at the lowest dose departed from what would be expected. Lastly, in a brain structure (striatum) involved in motor control, $C_{max}$ for NLX-112 was about half that for total CSF, and quite close to the free plasma concentrations. $T_{max}$ values were equivalent to those for total CSF at the two higher doses; $AUC_{0\text{-last}}$ values were similar to those observed for free plasma.

Quantitative analysis of the AUCs of concentrations of NLX-112 in all four tissues revealed that there was a highly linear and significant (all $F(1,1) > 192.4$, all $p < 0.01$) relationship between the dose of NLX-112 and its exposure level (supplementary Fig. 1).

### In vivo occupancy of brain 5-HT$_{1A}$ receptors by NLX-112 (microPET imaging)

Intravenous injection of $^{18}$F-F13640 (i.e., $^{18}$F-NLX-112) produced a distinctive pattern of binding to brain 5-HT$_{1A}$ receptors (see images of a representative rat, Fig. 2, panel A), with regions in red (corresponding to highest uptake)

**Table 1** Pharmacokinetic parameters of NLX-112 in rat brain and plasma

| | Total plasma | | | Free plasma | | | Total CSF | | | Free striatal ECF | | |
|---|---|---|---|---|---|---|---|---|---|---|---|---|
| *NLX-112 dose (mg/kg, i.p.)* | *0.04* | *0.16* | *0.63* | *0.04* | *0.16* | *0.63* | *0.04* | *0.16* | *0.63* | *0.04* | *0.16* | *0.63* |
| $C_{max}$ | 7.6 | 44.9 | 282.6 | 0.13 | 0.76 | 4.0 | 0.31 | 2.4 | 18.7 | 0.15 | 1.1 | 3.9 |
| $T_{max}$ | 0.5 | 0.25 | 0.25 | 0.5 | 1 | 1 | 0.5 | 0.25 | 0.25 | 1.75 | 1.25 | 1.25 |
| $T_{1/2}$ | 1.63 | 0.91 | 0.87 | 3.09 | 1.96 | 1.88 | 13.18 | 1.11 | 0.91 | 1.42 | 1.40 | 0.95 |
| $AUC_{0\text{-last}}$ | 11.5 | 75.1 | 360.0 | 0.3 | 2.0 | 10.9 | 0.8 | 3.8 | 24.9 | 0.4 | 2.5 | 8.0 |

NLX-112 levels were measured in plasma (total and free), in cerebrospinal fluid (CSF) and in striatal extracellular fluid (ECF)

$C_{max}$: Maximal concentration observed (ng/mL for plasma; ng/g for brain)

$T_{max}$: Time at which maximal concentration is observed (h)

$T_{1/2}$: Terminal phase half-life. The time it takes for the concentration levels to fall by 50% of their value (h)

$AUC_{0\text{-last}}$: Area under the concentration–time curve up to the last measurable concentration (ng.h/mL for plasma; ng.h/g for brain)

UNCORRECTED PROOF



Journal : Large 210 | Article No : 3323 | Pages : 12 | MS Code : 3323 | Dispatch : 29-7-2024

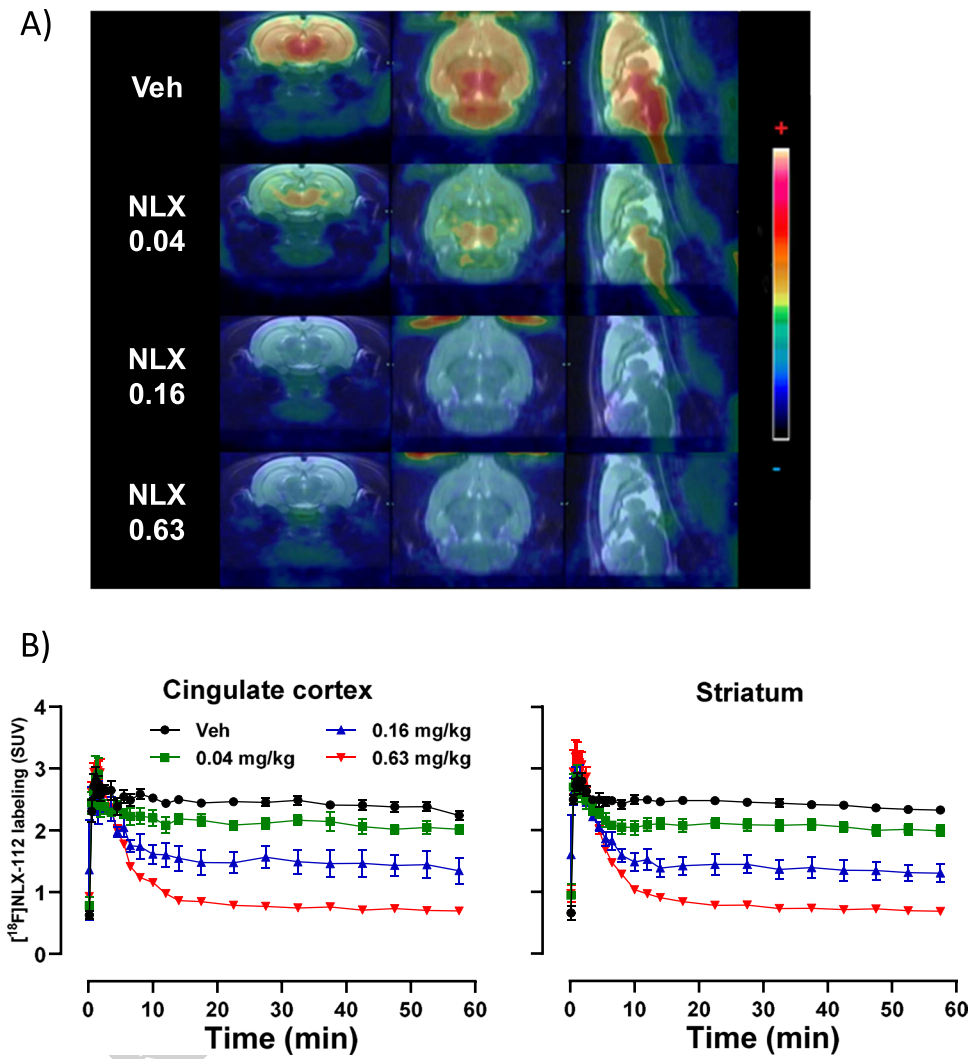


**Fig. 2** Occupancy of rat brain 5-$HT_{1A}$ receptors by NLX-112. Panel **A**: Coronal, transverse and sagittal representative summed microPET images on corresponding MRI rat brain template, showing $^{18}$F-F13640 (i.e., $^{18}$F-NLX-112) labeling in rat brain after pre-injection of vehicle (saline) or increasing doses of unlabeled NLX-112 (same scale used for all images). Panel **B**: Time course of the Standardized Uptake Values (SUVs) following administration of vehicle or NLX-112 (0.04, 0.16 or 0.63 mg/kg i.p.). Symbols are the mean ± SEM. Saline or NLX-112 were injected i.p. 30 min prior to the start of the microPET image acquisition (immediately before i.v. injection of $^{18}$F-F13640). N = 3–4 rats per treatment

localized mainly in the brainstem, thalamus and cortex. Treatment with unlabeled NLX-112, 30 min i.p. before the i.v. injection of $^{18}$F-F13640, dose-dependently reduced $^{18}$F-F13640 binding, as illustrated by a shift towards the blue color (corresponding to lowest uptake) in all brain regions examined. In other words, NLX-112 competed with $^{18}$F-F13640 for binding to the target 5-$HT_{1A}$ receptors.

Quantitative analysis of the competition between $^{18}$F-F13640 and unlabeled NLX-112 in the striatum and cingulate cortex confirmed that NLX-112 produced a robust dose-dependent reduction of the radiotracer uptake, that was readily observed after the initial peak 10 min after the start of microPET image acquisition, time at which the radiotracer uptake reached a plateau (Fig. 2, panel B). When averaging the last six frames of acquisition for the striatum and the cingulate cortex, the reduction was 14% and 13% at 0.04 mg/kg, 43% and 40% at 0.16 mg/kg and 70% and 70% at 0.63 mg/kg, respectively. Similar data were observed for 2 other brain regions examined (hippocampus and brain stem; data not shown). The analysis of occupancy of 5-$HT_{1A}$ receptors by unlabeled NLX-112, as estimated by the Lassen plot approach using the SUV uptake values in the different ROIs, yielded occupancy values of 11%, 64% and 93% at doses of 0.04, 0.16 and 0.63 mg/kg, respectively.

## Relationship between the in vivo occupancy of 5-$HT_{1A}$ receptors by NLX-112 andits anti-dyskinetic activity

Previous studies showed that NLX-112 dose-dependently reduced abnormal involuntary movements (AIMs, a rodent analog of LID) in hemi-parkinsonian rats with a unilateral 6-OHDA lesion of the striatum and chronically treated with L-DOPA to produce LID (Iderberg et al. 2015). Here we show that there is a relationship between increased in vivo occupancy of central 5-$HT_{1A}$ receptors by NLX-112 (present microPET imaging data), and its efficacy to decrease AIMs (behavioral data extracted from Fig. 3 in (Iderberg et al. 2015)). Hence, in rats treated with vehicle,

UNCORRECTED



Journal : Large 210 | Article No : 3323 | Pages : 12 | MS Code : 3323 | Dispatch : 29-7-2024

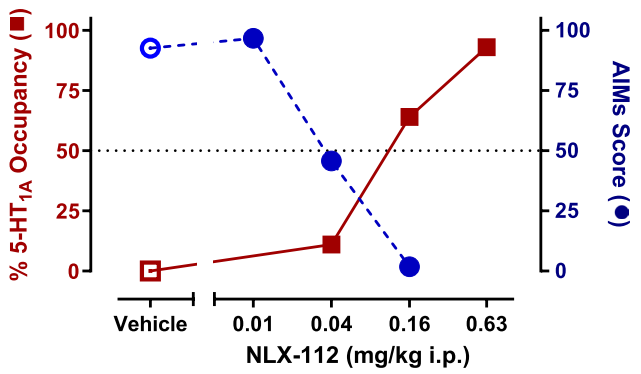


**Fig. 3** Anti-dyskinetic activity of NLX-112 correlated to its occupancy of rat striatal 5-$HT_{1A}$ receptors. Symbols are the mean. Data for striatal 5-$HT_{1A}$ receptors occupancy are from the $^{18}$F-NLX-112 microPET imaging experiment described herein. Data for the anti-dyskinetic activity of NLX-112 are adapted from (Iderberg et al. 2015) using the AIMs (Abnormal involuntary movements) scale for observation of rat behavior over a 3 h period. The dose of 0.63 mg/kg i.p. was not tested for anti-AIMS activity. The $ED_{50}$ for reduction of AIMs is approximately 0.04 mg/kg, corresponding to a total plasma exposure of 11.5 ng.h/ml (see AUC data in Table 1). The $ED_{50}$ for receptor occupancy is approximately 0.1 mg/kg, corresponding to a total plasma exposure of about 50 ng.h/ml

L-DOPA (6 mg/kg s.c.) elicits a high AIMs score (92.6), which is dose-dependently decreased as the occupancy of 5-$HT_{1A}$ receptors by NLX-112 increases. At the dose of 0.16 mg/kg i.p., at which there is a near total disappearance of AIMs (score reduced from 92.6 to 1.8), the occupancy of 5-$HT_{1A}$ receptors was 64%. A robust anti-LID activity (approximate halving of AIMs score) can be observed with a moderate (11%) level of occupancy of 5-$HT_{1A}$ receptors elicited by NLX-112 at 0.04 mg/kg i.p..

## Absence of pharmacokinetic interaction between NLX-112 & L-DOPA

Co-administration of NLX-112 (0.16 mg/kg i.p.) with L-DOPA (6 mg/kg s.c.; together with benserazide, 12 mg/kg s.c.) had no discernible influence on the plasma and brain concentrations of either NLX-112 or L-DOPA alone. Concentration versus time curves for NLX-112 and L-DOPA, whether for NLX-112 or L-DOPA administered alone, or for their combined administration (L-DOPA + NLX-112), were quasi superimposable, both for plasma and brain (Fig. 4). Examination of calculated PK parameters confirms this lack of interaction, for all four parameters examined: $C_{max}$, $T_{max}$, $T_{1/2}$, $AUC_{0\text{-last}}$ and $AUC_{0\text{-last}}$ Ratio (the ratio of the $AUC_{0\text{-last}}$ from the brain divided by that of the plasma) for compounds alone, or when combined (Table 2). As a reminder, this experiment was done to verify that the reduction of AIMs by NLX-112 in the rat LID model is not associated with changes in brain levels of L-DOPA.

## NLX-112 is neither an inhibitor nor a substrate at 8 drug transporters

NLX-112 was very weakly active as an inhibitor of 8 transporters (PgP, BCRP, OATP1B1, OATP1B3, OCT1, OCT2, OAT1, OAT3), including some that are located on the blood–brain barrier (BBB). $IC_{50}$ values ranged from 9.8 µM to over 100 µM (Supplementary Table 1). As a reminder, at doses active in rat motor disorders models (0.04 to 0.63 mg/kg i.p.), the corresponding free plasma $C_{max}$ of NLX-112 is in the range of 0.3 to 10.2 ng/ml, i.e., concentrations of 0.75 to 25.5 nM. These therapeutically relevant concentrations are therefore at least 1000-fold lower than the $IC_{50}$ values listed above. NLX-112, tested as a substrate, also showed

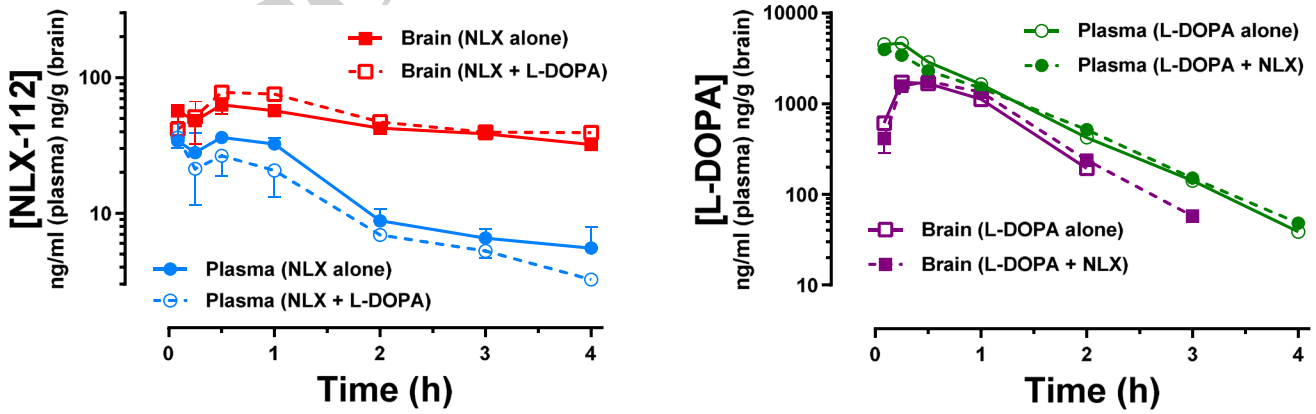


**Fig. 4** Absence of pharmacokinetic interaction between NLX-112 and L-DOPA. Symbols are the mean and SEM of drug concentrations, expressed in ng/ml (for plasma) or ng/g (for brain). Note that the X axes scales are logarithmic. L-DOPA (6 mg/kg s.c.) was co-administered with the L-decarboxylase blocker benserazide (12 mg/kg s.c.); NLX-112 was administered at 0.16 mg/kg i.p.. N = 3 rats per point

CORRECTED PROOF



Journal : Large 210 | Article No : 3323 | Pages : 12 | MS Code : 3323 | Dispatch : 29-7-2024

**Table 2** PK parameters of NLX-112 and L-DOPA administered alone or in combination

| | NLX-112 | | | | L-DOPA | | | |
|---|---|---|---|---|---|---|---|---|
| | NLX-112 Alone | | With L-DOPA | | L-DOPA Alone | | With NLX-112 | |
| | Plasma | Brain | Plasma | Brain | Plasma | Brain | Plasma | Brain |
| $C_{max}$ | 36.3 | 63.1 | 36.2 | 78.1 | 4640 | 1715 | 3967 | 1763 |
| $T_{max}$ | 0.0833 | 0.50 | 0.50 | 0.50 | 0.25 | 0.25 | 0.0833 | 0.50 |
| $T_{1/2}$ | 1.13 | 3.61 | 1.17 | 3.11 | 0.56 | 0.47 | 0.59 | 0.44 |
| $AUC_{0\text{-last}}$ | 48.3 | 180.6 | 66.2 | 208.2 | 4423 | 1998 | 3875 | 2310 |
| Brain:Plasma Ratio | 3.74 | | 3.15 | | 0.45 | | 0.60 | |

NLX-112 was administered i.p. at 0.16 mg/kg; L-DOPA was administered s.c. at 6 mg/kg, with 12 mg/kg s.c. benserazide

$C_{max}$: Maximal concentration observed (ng/mL for plasma; ng/g for brain)

$T_{max}$: Time at which maximal concentration is observed (h)

$T_{1/2}$: Terminal phase half-life (time for the concentration levels to fall by 50% of their value, in h)

$AUC_{0\text{-last}}$: Area under the concentration–time curve up to the last measurable concentration (ng.h/mL for plasma; ng.h/g for brain)

Brain:Plasma Ratio: Based on the $AUC_{0\text{-last}}$ from the brain divided by that of the plasma

essentially negligible interaction with these 8 transporters, (Supplementary Table 2. Altough the maximal concentration tested for the first two transporters was 2 µM (as opposed to 100 µM for the others), the results indicate that there is at least a 100-fold separation versus therapeutically relevant concentrations of NLX-112 (see above). It is therefore very unlikely that NLX-112 will block or act as a substrate for these drug transporters, at least as concerns those present at the level of the BBB. INSERT SECTION HEAD HERE

The present study of NLX-112, combining pharmacodynamic, pharmacokinetic and brain imaging data in rats, shows that, following acute systemic administration: 1) NLX-112 exposure in plasma and brain peaks rapidly and is observed for an extended period of time; 2) NLX-112 occupies brain 5-$HT_{1A}$ receptors at pharmacologically-relevant doses; 3) a moderate level of brain 5-$HT_{1A}$ receptors occupancy is sufficient to efficaciously reduce the AIMS score (a rat readout of LID) and 4) NLX-112 does not modify the plasma and brain pharmacokinetic profile of L-DOPA (and vice-versa).

## NLX-112 plasma and brain exposure at pharmacological doses

The present study shows that NLX-112 rapidly penetrates the brain following systemic administration and that it has an extended half-life therein. Thus, at a dose of 0.63 mg/kg i.p., total plasma NLX-112 reached a $C_{max}$ of 282.6 ng/mL within 15 min, with levels dropping by about 90% at 3 h. This is similar to values obtained in a previous rat PK study (Bardin et al. 2005) where, at the same dose of 0.63 mg/kg i.p., total plasma $C_{max}$ was 293.4 ng/mL with a $T_{max}$ of 15 min, and a decrease of about 90% at 4 h. It is notable that the rapid absorption to plasma of NLX-112 is also seen in higher species: in marmosets, total plasma $C_{max}$ at a dose of 0.4 mg/kg p.o. at 1 h was 254.6 ng/ml and decreased by around 80% at 4 h (Fisher et al. 2020). In macaques, total plasma $C_{max}$ of NLX-112 at a dose of 0.1 mg/kg p.o. was 50.6 ng/mL at 30 min, with levels dropping by around 90% at 4 h (Depoortere et al. 2020). The PK parameters of NLX-112 have also been explored in humans: a single 1 mg oral dose of NLX-112 as an immediate-release tablet produced a total plasma $C_{max}$ of 22 ng/mL at a Tmax of 2 h (Paillard et al. 2016). Overall, the data from all the species indicate consistently rapid absorption properties of NLX-112 with substantial exposure in blood plasma.

In addition to rapid absorption in plasma, the present data also point to rapid and robust brain penetration at levels that are sufficient to bind to 5-$HT_{1A}$ receptors. This conclusion is supported by the free striatal ECF levels of NLX-112 at a pharmacologically meaningful dose of 0.16 mg/kg (range: 0.4–1.1 ng/mL, i.e. 1.0 to 2.8 nM). These are slightly above the binding affinity of NLX-112 for the rat 5-$HT_{1A}$ receptor (Ki = 0.85 nM) (Newman-Tancredi et al. 2017), suggesting that, when NLX-112 is administered at that dose, it produces free brain concentrations that are sufficient to bind and activate 5-$HT_{1A}$ receptors and thereby elicit complete suppression of AIMs in the rat model of LID (Iderberg et al. 2015). It should be noted that the brain concentrations measured here for striatum (3.9 ng/mL at a dose of 0.63 mg/kg i.p.) are similar to those reported previously for rat hippocampus (3.6 ng/mL also at 0.63 mg/kg i.p.), using similar analyses from hippocampal microdialysate samples (Bardin et al. 2005). Moreover the two studies found similar $T_{max}$ values of 1 h for the hippocampus (Bardin et al. 2005)), and 75 min herein for the striatum. This suggests that NLX-112

UNCORRECTED PROOF



Journal : Large 210 | Article No : 3323 | Pages : 12 | MS Code : 3323 | Dispatch : 29-7-2024

distributes uniformly in brain and is able to engage its molecular target (i.e., 5-$HT_{1A}$ receptors) in different brain regions (see further comments below).

## Relationship between brain 5-$HT_{1A}$ receptor occupancy and anti-dyskinetic activity in rats

The availability of $^{18}$F-F13640 (i.e., $^{18}$F-NLX-112), a radiolabeled form of NLX-112, enables direct measurement of its distribution in rat brain by PET imaging, as also previously done in cats and NHP (Vidal et al. 2018) and in humans (Colom et al. 2020; Courault et al. 2023). This allows investigation of the occupancy of functionally active population of 5-$HT_{1A}$ receptors. This is a critical point because previous PET studies using classical antagonist radiotracers of 5-$HT_{1A}$ receptors failed to detect significant occupancy by 5-$HT_{1A}$ agonists at pharmacologically active doses, a finding which is likely due to the presence of only a low proportion of active state receptors out of the total receptor population (Bantick et al. 2004). Previous work with $^{18}$F-NLX-112 showed that it very rapidly penetrates the brain and specifically labels 5-$HT_{1A}$ receptors with an extended half-life in rat, cat, macaque and human subjects (Vidal et al. 2018) (Colom et al. 2020; Courault et al. 2023).

Here, unlabeled NLX-112 dose-dependently inhibited $^{18}$F-F13640 binding, with near-maximal occupancy being observed at 0.63 mg/kg. This profile was essentially identical across all brain regions examined, providing further evidence that NLX-112 can interact with 5-$HT_{1A}$ receptors in different brain regions with the same dose–response relationship. Importantly, as well as demonstrating target engagement, these data enable estimation of central occupancy of functional 5-$HT_{1A}$ receptors necessary for therapeutic-like effects. Thus, even a modest occupancy of active-state 5-$HT_{1A}$ receptors was sufficient to elicit robust antidyskinetic activity. Indeed, the NLX-112 dose of 0.04 mg/kg i.p, which has been previously shown to diminish AIMs by about half (Iderberg et al. 2015), produced occupancy of only 11%, whereas the dose of 0.16 mg/kg i.p. occupied 60–70% of active-state 5-$HT_{1A}$ receptors in brain, and thereby elicited complete suppression of AIMs in the rat model of LID. This suggests that active-state 5-$HT_{1A}$ receptors are highly sensitive to agonist stimulation, at least in the case of a full agonist such as NLX-112. It should be noted, however, that changes in 5-$HT_{1A}$ receptor expression and sensitivity occur upon lesioning of dopaminergic neurons and upon repeated L-DOPA administration (Chaib et al. 2023; Vidal et al. 2021), so these findings would benefit from further investigation using 'hemi-parkinsonian' rats (i.e., with unilateral 6-OHDA lesions of the Substantia nigra, a rodent model of LID).

## Absence of PK interaction between NLX-112 and L-DOPA

The presence of NLX-112 did not influence the levels of L-DOPA, whether in the plasma or in the whole brain. This is important because the reduction of AIMs in hemi-parkinsonian rats by NLX-112 could be hypothesized to be consecutive to a reduction in available L-DOPA. The absence of a pharmacokinetic interaction, both peripherally and centrally, therefore supports the conclusion that the potent and efficacious anti-LID activity of NLX-112 stems from a genuine pharmacodynamic phenomenon, mediated by NLX-112's activation of central 5-$HT_{1A}$ receptors (rather than by a decrease in levels of L-DOPA). This is consistent with the observation that the anti-LID effects of NLX-112 are abolished by a selective 5-$HT_{1A}$ receptor antagonist, WAY100,635 (Iderberg et al. 2015), indicating specific target interaction.

## Limitations of the study

Some limitations of the present study should be noted. Firstly, the PK profile of NLX-112 was investigated in male rats and might differ in female rats. However, a pilot PK study in female Sprague–Dawley rats showed that, at a NLX-112 dose of 0.63 mg/kg i.p., total plasma $C_{max}$ was 301 ng/mL with $T_{max}$ at 30 min (Neurolixis unpublished data) which is similar to values reported in Table 1 for males of the same strain ($C_{max}$ 282.6 ng/mL, $T_{max}$ 15 min), suggesting that there is no sex difference in PK parameters. Secondly, the present study tested only acute administration of NLX-112 and it would be valuable to conduct PK studies following a protracted treatment (e.g., 2–3 weeks) with NLX-112, to determine whether there is drug accumulation in particular brain regions. Lastly, the present studies were conducted in 'normal' rats, and it would be informative to conduct experiments in hemi-parkinsonian rats that have been subjected to a protracted treatment with L-DOPA to produce LID, as mentioned above.

## Conclusions and perspectives

To summarize, NLX-112 presents a PK profile in rats highly compatible with that of drugs developed for pharmacotherapeutic treatment of CNS diseases. Indeed, following acute i.p. treatment at pharmacologically relevant doses, NLX-112 rapidly penetrates its target tissue (the brain), where it remains detectable for several hours and with a high target engagement of central 5-$HT_{1A}$ receptors, as assessed by microPET brain imaging. Furthermore, based on total exposure (Table 2) its brain:plasma AUC ratio is high (almost 4), a favorable property for a drug under development for treatment of CNS disorders (although the ratio between free striatal and free plasma

UNCORRECTED PROOF



Journal : Large 210 | Article No : 3323 | Pages : 12 | MS Code : 3323 | Dispatch : 29-7-2024

concentrations, i.e. Kp,uu values, have not been assessed). Lastly, there is no detectable PK interaction between NLX-112 and L-DOPA, whether in brain or plasma, indicating that the two compounds can be assessed independently for dosing purposes. These findings support the further development of NLX-112 for the treatment of LID, notably following the recent positive phase 2a clinical trial in PD patients, which met both its primary outcome of safety and tolerability, and secondary outcomes of efficacy against both LID and parkinsonian motor disability (Svenningsson et al. 2023). Nevertheless, further PK and 5-$HT_{1A}$ receptor occupancy studies in human subjects would be useful to establish the extent to which the present observations in rat translate to a clinical context.

**Supplementary Information** The online version contains supplementary material available at https://doi.org/10.1007/s00210-024-03323-0.

**Authors contribution** All authors have approved the final version of the manuscript and declare that all data were generated in-house and that no paper mill was used. Ronan Depoortere: Data interpretation; Writing: original draft, review & editing. Andrew C. McCreary: Conceptualization, Data curation, Formal analysis, Visualization, Writing: review & editing. Benjamin Vidal: Conceptualization, Data curation, Formal analysis, Visualization, Writing: review & editing. Luc Zimmer: Conceptualization, Data curation, Formal analysis, Visualization, Writing: review & editing. Mark Varney: Conceptualization, Data interpretation, Visualization, Writing: review & editing. Adrian Newman-Tancredi: Conceptualization, Data interpretation, Visualization, Writing: review & editing.

**Funding** Financial support for pharmacokinetic studies was received from the Michael J. Fox Foundation for Parkinson's Research (grant ID# 9233). The microPET study was supported by the LABEX PRIMES (ANR-11-LABX-0063) of Université de Lyon and the 'Investissements d'Avenir' program (ANR-11-IDEX-0007) from the French National Research Agency (ANR) and the imaging platform, CERMEP (Lyon, France).

**Data availability** Data supporting the findings of this study are available within the paper and its Supplementary Information.

## Declarations

**Ethical approval** ANT, MAV and RYD are shareholders and/or employees of Neurolixis. The other authors declare no competing interests.

## References

Bantick RA, Rabiner EA, Hirani E et al (2004) Occupancy of agonist drugs at the 5-HT1A receptor. Neuropsychopharmacology : Official Publication of the American College of Neuropsychopharmacology 29(5):847–859

Bardin L, Assie MB, Pelissou M et al (2005) Dual, hyperalgesic, and analgesic effects of the high-efficacy 5-hydroxytryptamine 1A (5-HT1A) agonist F 13640 [(3-chloro-4-fluoro-phenyl)-[4-fluoro-4-{[(5-methyl-pyridin-2-ylmethyl)-amino]-me thyl} piperidin-1-yl]methanone, fumaric acid salt]: relationship with 5-HT1A receptor occupancy and kinetic parameters. J Pharmacol Exp Ther 312(3):1034–1042

Barnes NM, Ahern GP, Becamel C et al (2021) International Union of Basic and Clinical Pharmacology. CX. Classification of Receptors for 5-hydroxytryptamine; Pharmacology and Function. Pharmacol Rev 73(1):310–520

Borroto-Escuela DO, Ambrogini P, Chruscicka B et al (2021) The Role of Central Serotonin Neurons and 5-HT Heteroreceptor Complexes in the Pathophysiology of Depression: A Historical Perspective and Future Prospects. Int J Mol Sci 22(4):1927

Caccia S, Muglia M, Mancinelli A et al (1983) Disposition and metabolism of buspirone and its metabolite 1-(2-pyrimidinyl)-piperazine in the rat. Xenobiotica 13(3):147–153

Celada P, Bortolozzi A, Artigas F (2013) Serotonin 5-HT1A receptors as targets for agents to treat psychiatric disorders: rationale and current status of research. CNS Drugs 27(9):703–716

Chaib S, Vidal B, Bouillot C et al (2023) Multimodal imaging study of the 5-HT(1A) receptor biased agonist, NLX-112, in a model of L-DOPA-induced dyskinesia. Neuroimage Clin 39:103497

Colom M, Costes N, Redoute J et al (2020) [18F]-F13640 PET imaging of functional receptors in humans. Eur J Nucl Med Mol Imaging 47(1):220–221

Colom M, Vidal B, Fieux S et al (2021) [(18)F]F13640, a 5-HT1A Receptor Radiopharmaceutical Sensitive to Brain Serotonin Fluctuations. Front Neurosci 15:622423

Courault P, Lancelot S, Costes N et al (2023) [(18)F]F13640: a selective agonist PET radiopharmaceutical for imaging functional 5-HT(1A) receptors in humans. Eur J Nucl Med Mol Imaging 50(6):1651–1664

Cunningham VJ, Rabiner EA, Slifstein M et al (2010) Measuring drug occupancy in the absence of a reference region: the Lassen plot re-visited. J Cereb Blood Flow Metab 30(1):46–50

Depoortere R, Johnston TH, Fox SH et al (2020) The selective 5-HT1A receptor agonist, NLX-112, exerts anti-dyskinetic effects in MPTP-treated macaques. Parkinsonism Relat Disord 78:151–157

Fisher R, Hikima A, Morris R et al (2020) The selective 5-HT1A receptor agonist, NLX-112, exerts anti-dyskinetic and anti-parkinsonian-like effects in MPTP-treated marmosets. Neuropharmacology 167:107997

Iderberg H, McCreary AC, Varney MA et al (2015) NLX-112, a novel 5-HT1A receptor agonist for the treatment of L-DOPA-induced dyskinesia: Behavioral and neurochemical profile in rat. Exp Neurol 271:335–350

Levigoureux E, Vidal B, Fieux S et al (2019) Serotonin 5-HT1A receptor biased agonists induce different cerebral metabolic responses: A [18F]FDG PET study in conscious and anesthetized rats. ACS Chem Neurosci 10(7):3108–3119

Newman-Tancredi A, Martel JC, Cosi C et al (2017) Distinctive in vitro signal transduction profile of NLX-112, a potent and efficacious serotonin 5-HT1A receptor agonist. J Pharm Pharmacol 69(9):1178–1190

Newman-Tancredi A, Depoortere RY, Kleven MS et al (2022) Translating biased agonists from molecules to medications: Serotonin 5-HT1A receptor functional selectivity for CNS disorders. Pharmacol Ther 229:107937

Pagano G, Niccolini F, Politis M (2017) The serotonergic system in Parkinson's patients with dyskinesia: evidence from imaging studies. J Neural Transm (vienna). https://doi.org/10.1007/s00702-017-1823-7

Paillard B, Del Frari L, Brunner V, et al. (2016) A method for treating movement disorders with befiradol. In: WO2016/005527A1 (ed).

Paxinos G, Watson C (2007) The Rat Brain in Stereotaxic Coordinates. Academic Press

Pourhamzeh M, Moravej FG, Arabi M, et al (2021) The Roles of Serotonin in Neuropsychiatric Disorders. Cell Mol Neurobiol.

UNCORRECTED PROOF

Epub ahead of print 2021/03/03. https://doi.org/10.1007/s10571-021-01064-9

Prinssen EP, Colpaert FC, Koek W (2002) 5-HT1A receptor activation and anti-cataleptic effects: high-efficacy agonists maximally inhibit haloperidol-induced catalepsy. Eur J Pharmacol 453(2–3):217–221

Svenningsson P, Odin P, Bergquist F, et al (2023) NLX-112 has favorable safety, tolerability and efficacy against levodopa-induced dyskinesia (LID) in a randomized, double-blind, placebo-controlled, proof-of-concept Ph2A study. In: World Parkinson's Congress, July 4–7, 2023, Barcelona, Poster Board #LBP38.31

Takano A, Gulyas B, Varnas K et al (2014) Low brain CB1 receptor occupancy by a second generation CB1 receptor antagonist TM38837 in comparison with rimonabant in nonhuman primates: a PET study. Synapse 68(3):89–97

Vidal B, Fieux S, Billard T et al (2014) Radiopharmacological evaluation of [18F]F13640, a novel 5-HT1A receptor agonist. J Nuclear Medicine 55(Supp. 1):1100

Vidal B, Fieux S, Colom M et al (2018) [18F]-F13640 preclinical evaluation in rodent, cat and primate as a 5-HT1A receptor agonist for PET neuroimaging. Brain Struct Funct 223(6):2973–2988

Vidal B, Bolbos R, Redoute J et al (2020) Pharmacological MRI to investigate the functional selectivity of 5-HT1A receptor biased agonists. Neuropharmacology 172:107867

Vidal B, Levigoureux E, Chaib S et al (2021) Different alterations of agonist and antagonist binding to 5-HT1A receptor in a rat model of Parkinson's disease and levodopa-induced dyskinesia : a microPET study. Journal of Parkinson Disease 11(3):1257–1269

**Publisher's Note** Springer Nature remains neutral with regard to jurisdictional claims in published maps and institutional affiliations.

Springer Nature or its licensor (e.g. a society or other partner) holds exclusive rights to this article under a publishing agreement with the author(s) or other rightsholder(s); author self-archiving of the accepted manuscript version of this article is solely governed by the terms of such publishing agreement and applicable law.

UNCORRECTED PROOF

| | |
|---|---|
| Journal: | **210** |
| Article: | **3323** |

# Author Query Form

**Please ensure you fill out your response to the queries raised below and return this form along with your corrections**

Dear Author

During the process of typesetting your article, the following queries have arisen. Please check your typeset proof carefully against the queries listed below and mark the necessary changes either directly on the proof/online grid or in the 'Author's response' area provided below

| Query | Details Required | Author's Response |
|---|---|---|
| AQ1 | Please check if the article title was captured and presented correctly. | |
| AQ2 | Please confirm if the authors names are presented accurately and in the correct sequence (extended given name, middle name/initial, family name). Also kindly confirm the details in the metadata are correct. | |
| AQ3 | Please check the provided affiliation if captured and presented correctly. | |
| AQ4 | Please check and confirm if section heads and subheads are assigned to appropriate levels. Otherwise, kindly amend. | |
| AQ5 | Please check if all figure captions are captured and presented correctly. | |
| AQ6 | Please check if the table captions, cell entries, and footnotes are captured and presented correctly. | |
| AQ7 | According to our submission guidelines for authors, first subsection "Important Submission Policy" (https://www.springer.com/journal/210/submissionguidelines#Instructions%20for%20Authors_Important%20Submission%20Policy), ALL papers must include the following statement in the section "Authors Contributions": The authors declare that all data were generated in-house and that no paper mill was used. This is not the case in your accepted article. Please confirm that we can add this sentence in the section "Authors Contributions". | |
| AQ8 | Please check if back matter sections are captured/presented correctly. Otherwise, kindly amend. | |
| AQ9 | Please check supplementary materials and information if captured and presented correctly. | |
| AQ10 | Please verify reference Borroto-Escuela et al., 2021 if captured and presented correctly. | |